
Yuto SAKUMA

LES analysis on atmospheric dispersion in urban area under various thermal conditions

Yuto Sakuma[1], Tomotaka Hosoi[2], Hidenori Kawai[3], Tetsuro Tamura[4]

1 Graduate Student, Tokyo Institute of Technology, Japan, sakuma.y.ae@m.titech.ac.jp
2 Former Graduate Student, Tokyo Institute of Technology, Japan, hosoi.t.ad@ m.titech.ac.jp
3 Research Associate, Tokyo Institute of Technology, Japan, kawai.h.ac@ m.titech.ac.jp
4 Professor, Tokyo Institute of Technology, Japan, tamura@depe.titech.ac.jp

1. INTRODUCTION

For keeping human health from the pollutant impact, it is important to predict accurately near ground high concentrations for atmospheric dispersion in urban area. However, the dispersion characteristics are sensitively changed by convective phenomena based on the wind flows above and within the urban canopy layers. The aspect of urban surface is very complicated by various roughness elements such as houses, vegetation and buildings. Also, in the center of a large city tall buildings are densely arrayed in the limited region of a few kilometers square. According to these aspects, different flow patterns like vortex shedding, separating shear flows or flow circulation, appear in the wake and determine the dispersion characteristics. Thus far, in order to classify and clarify these characteristics, many studies about atmospheric dispersion considering the detailed configuration of city have been carried out [(1), (2)]. But almost all of them were under the neutral condition for atmosphere and did not deal with the effects of waste heat from buildings. Studies on pollutant dispersion considering the thermal stability of the ambient wind or flows in the urban canopy are very rare in these days.

This study tries to carry out Large Eddy simulation (LES) which reveals the occurrence of high concentration by local flow phenomena such as cavity flows and separation around the surface obstacles. Also, taking into consideration great change of peak occurrence by the combined effect of atmospheric stability and local building waste heat over the roughened surface by dense buildings, its dispersion mechanism are investigated. Local thermal impact by temperatures of building wall and roofs produces a stratification effect separately from atmospheric stability, and give a change in turbulent flow phenomena above and within the urban canopy. Accordingly, this study understands the exact concentration field, which needs to consider rough wall effect, atmospheric stability effect as a background, local heating effect from building wall. In order to elucidate such a specific urban dispersion process for safety and comfort of atmospheric environment, this study aims at obtaining the knowledge on detailed unsteady flow patterns accompanied with complex behavior.

In this paper, an urban model is constructed using simple roughness block, which has the thermal boundary condition on building wall. Considering actual phenomena in cities, atmospheric stability is imposed in the computational domain. LES of atmospheric diffusion over urban roughness block elements is performed. In addition, the analysis on the obtained results focuses on the turbulent energy exchange between above and within the unban canopy, in order to clarify the generating, the developing or the decaying process of coherent structures such as vortices above urban canopy, updraft or downdraft inside canopy. Also, their flow visualization can exhibit roles of coherent structures for occurrence of high concentration. Finally, we conclude that above information makes a contribution to safety and comfort for human society.

2. ANALYTICAL METHOD

2.1 Governing equation for Large Eddy Simulation

The turbulent flow in this simulation is calculated by large eddy simulation (LES). The governing equations of LES are given as follows, i.e., the continuity equation, incompressible Navier-Stokes equation, momentum equations of temperature and diffusion shown in Eq. (1)-(7).

$$\frac{\partial \overline{u_i}}{\partial x_i} = 0 \tag{1}$$

$$\frac{\partial \overline{u_i}}{\partial t} + \frac{\partial \overline{u_i}\,\overline{u_j}}{\partial x_j} = -\frac{1}{\rho_0}\frac{\partial \overline{p}}{\partial x_i} + \frac{\partial}{\partial x_j}\nu\left(\frac{\partial \overline{u_i}}{\partial x_j} + \frac{\partial \overline{u_j}}{\partial x_i}\right) + \mathrm{g}\beta\overline{\theta}\delta_{i2} - \frac{\partial \tau_{ij}}{\partial x_j} + \delta(b)f \tag{2}$$

$$\frac{\partial \overline{\theta}}{\partial t} + \frac{\partial \overline{\theta}\,\overline{u_j}}{\partial x_j} = \frac{\partial}{\partial x_j}\left(\alpha\frac{\partial \overline{\theta}}{\partial x_j}\right) - \frac{\partial h_j}{\partial x_j} + \delta(b)f \tag{3}$$

$$\frac{\partial \overline{c}}{\partial t} + \frac{\partial \overline{c}\,\overline{u_j}}{\partial x_j} = \frac{\partial}{\partial x_j}\left(\kappa\frac{\partial \overline{c}}{\partial x_j}\right) - \frac{\partial s_j}{\partial x_j} + \delta(b)f \tag{4}$$

$$\tau_{ij} = \overline{u_i u_j} - \overline{u_i}\,\overline{u_j} \tag{5}$$

$$h_j = \overline{\theta u_j} - \overline{\theta}\,\overline{u_j} \tag{6}$$

$$s_j = \overline{c u_j} - \overline{c}\,\overline{u_j} \tag{7}$$

$$\mathrm{Re} = \frac{LU}{\nu}, \quad \mathrm{Ri} = \beta\frac{\Delta\Theta L}{U^2} \quad \mathrm{Pr} = \frac{\nu}{\alpha}, \quad \mathrm{Sc} = \frac{\nu}{\kappa} \tag{8}$$

where, u_i is the velocity, θ is the temperature, c is the concentration, t is the time, ρ is the density, p is the pressure, β is the thermal expansion coefficient and g is the gravity acceleration. Moreover, the non-dimensional parameters which will be used in the following sections are shown in Eq. (8), i.e., Re (Reynolds number), Pr (Prandtl number) and Sc (Schmidt number). The Boussinesq approximation is employed in order to consider the buoyancy effect by heat. τ_{ij}, h_j and s_j are the subgrid-scale (SGS) Reynolds stress, heat flux and scalar flux respectively, and represented by the eddy viscosity concept as follows:

$$\tau_{ij} - \frac{1}{3}\delta_{ij}\tau_{ij} \approx -2\nu_{sgs}\overline{S_{ij}}, \qquad \overline{S_{ij}} = \frac{1}{2}\left(\frac{\partial \overline{u_i}}{\partial x_j} + \frac{\partial \overline{u_j}}{\partial x_i}\right) \tag{9}$$

$$\nu_{sgs} = (C_s\Delta)^2(2\overline{S_{ij}}\,\overline{S_{ij}})^{1/2} \tag{10}$$

$$h_j = -\alpha_{sgs}\frac{\partial \overline{\theta}}{\partial x_j}, \qquad \alpha_{sgs} = \frac{\nu_{sgs}}{Pr_{sgs}} \tag{11}$$

$$s_j = -\kappa_{sgs}\frac{\partial \overline{c}}{\partial x_j}, \qquad k_{sgs} = \frac{\nu_{sgs}}{Sc_{sgs}} \tag{12}$$

In this simulation, we used the Smagorinsky model for turbulent equation, Gradient diffusion approximation model for temperature and diffusion equation. Van Driest function is used for damping the turbulent viscosity near the wall. The constant number of SGS modelling is set as follows; Cs=0.1, Pr_{sgs}=0.6, Sc_{sgs}=0.5. Finite differences calculation for numerical method, Fractional-Step method computational algorithm, SOR method for iterative solution of pressure equation and Staggered grid for computation grid is used.

Fig. 2.1 shows the general description of this study. Inflow of urban area is adequately developed, it include the roughness effect of surface geometry and thermal stratification of atmospheric boundary layer. In order to reproduce these characteristics, we separate the computational domain as three regions; spatial development section (Driver region 1), stratification effect section (Driver region 2), diffusion analysis section (Driver region 3), and add the each effect to turbulent boundary layer.

To generate the inflow turbulence, we used the Nozawa's method [3] which is effective to simulate the turbulent boundary layer include the roughness. Nozawa's method expands Lund's method [4] for roughness boundary layer. In Lund's method, the velocity at recycle point is rescaled, and then re-introduced as an inlet boundary condition. This method allows calculating the spatially developing boundary layer conducting with qwasi-periodic boundary conditions which applied in the stream wise direction.

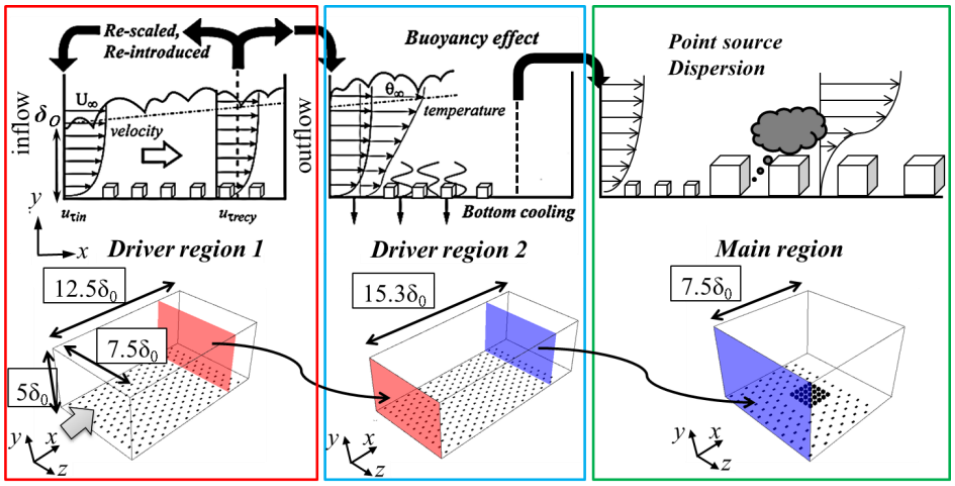

Fig. 2.1 Numerical model for rough wall turbulent boundary layer

2.2 Modeling for boundary surface with roughness blocks

Fig. 2.2 shows the modeling of roughness block in this study. In order to presenting the roughness elements on the boundary surface, we adopted the method called feedback-forcing which proposed by Goldstein and Sirovich [5] where the variable external force is given by the feedback from the difference between the specified velocity and the velocity in the computation. In this method, the external force at the point (time t and coordinate position x) within the flow field is calculated by (13), where $u(x,t)$ is the velocity at the point, $u_0(x,t)$ is a specified velocity and α, β are appropriate negative parameters. This method has an advantage in the ease in computation because only the addition of the external force term enables to give a specified velocity in the flow and thus to calculate similarly through whole computational domain.

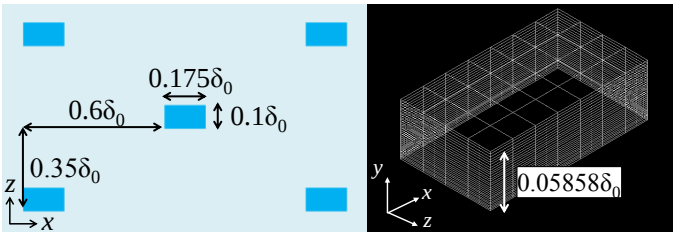

Fig. 2.2 modeling of roughness blocks

$$f(\boldsymbol{x},t) = \alpha\int_0^t \big(\boldsymbol{u}(\boldsymbol{x},t) - \boldsymbol{u_0}(\boldsymbol{x})\big)dt + \beta(\boldsymbol{u}(\boldsymbol{x},t) - \boldsymbol{u_0}(\boldsymbol{x})) \tag{13}$$

3. NUMERICAL VALIDATION FOR SPATIALLY DEVELOPING TURBULENT BOUNDARY LAYER

In this section, we validate the numerical simulation model for plume dispersion in the thermally-stratified boundary layers. Fig. 3.1 shows the inflow condition include the thermal stratification effect.

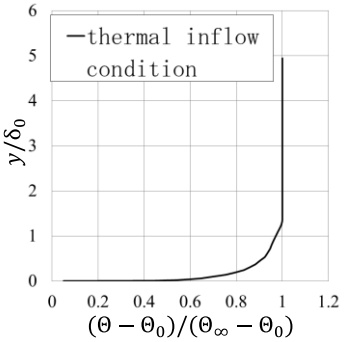

Fig. 3.1 Thermal inflow

3.1 Validation for physical model of roughness blocks

Firstly, we compare the present numerical results with Schultz's experimental results at Fig. 3.2 [6] (red line means numerical results), to validate the physical adequacy of inflow turbulence of roughness blocks that is modeled by feedback-forcing technique. It can be seen that a good consistency is achieved and the roughness blocks are effective for creating the inflow turbulence. In addition, we compare the average velocity field and turbulent intensity of streamwise velocity with Load Recommendation for Building Design [7] at Fig. 3.3, confirming the agreement of power low relationship between this study and atmospheric boundary layer at real urban canopy layer with roughness classification No. 4 (α=0.27). It can be concluded that present numerical model with roughness blocks succeeds in simulating the atmospheric boundary layer at real urban canopy layer.

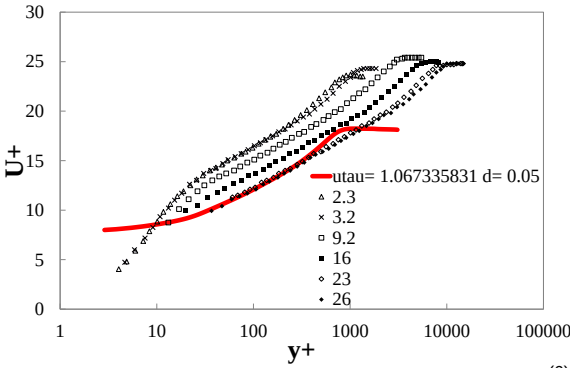

Fig. 3.2 Comparison with Schultz's experiment [6]

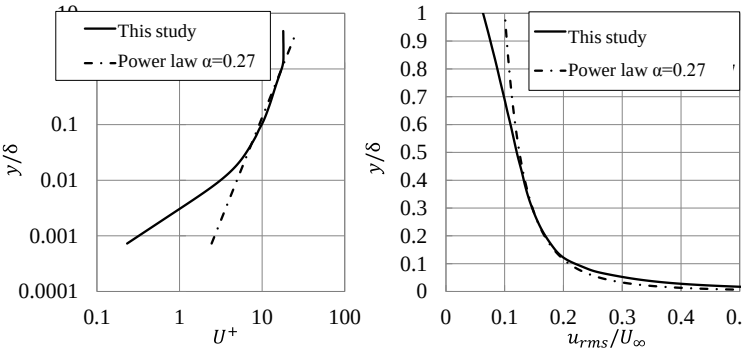

Fig. 3.3 Comparison with Loads on Buildings [7]

3.2 Validation for thermal stratification effect

Secondly, Ohya's S3 experimental results are used to make validation of thermal stratification effect as shown in at Fig. 3.4 [8]. Table 3.1 shows the conditions of the experiment and this study which has smooth and rough boundary condition with thermal stratification effect. Based on comparison of mean temperature, mean velocity and fluctuation intensity, tendencies are not different, but in Reynolds stress there is a peak in both rough cases at the nearly same height (red arrow). There is some distinction on roughness condition but generative mechanism of turbulence on rough cases is more similar than smooth case. From this validation, turbulent structure is also maintained by appropriate roughness settings in thermal stratification effect.

Table 3.1 calculation and experimental condition

	δ_{inflow}	$Re\delta_{inflow}$	$Ri\delta_{inflow}$	$\delta_{x=12.4}$	$Re\delta_{x=12.4}$	$Ri\delta_{x=12.4}$
Smooth	1.03	11,748	0.30	1.02	11693	0.29
Rough	1.36	20,335	0.38	1.03	15,456	0.29
Ohya S3					46,000	0.39

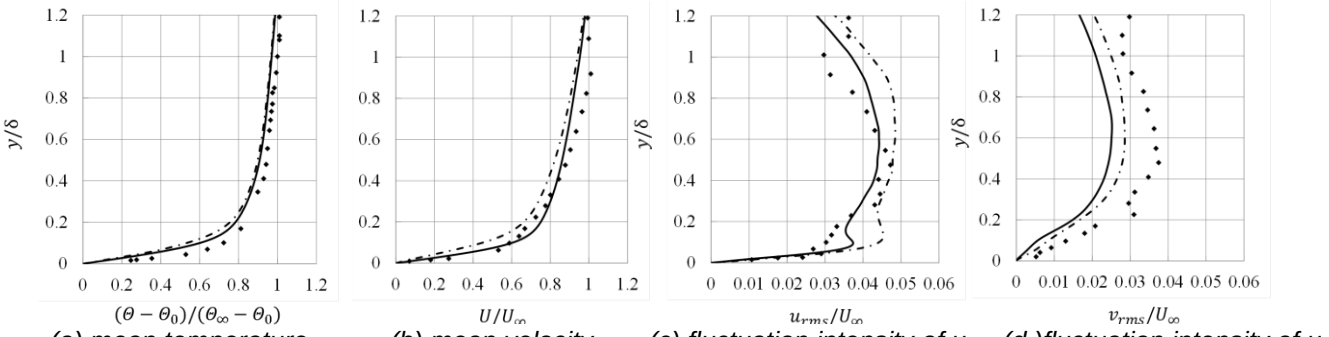

(a) mean temperature *(b) mean velocity* *(c) fluctuation intensity of u* *(d)fluctuation intensity of u*

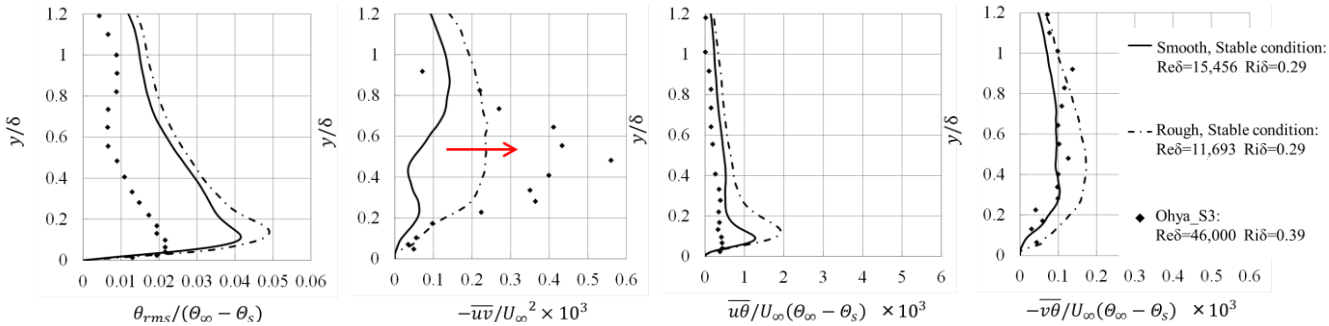

(e) fluctuation intensity of Θ *(f) Reynolds stress* *(g) thermal flux of x* *(h) thermal flux of y*

Fig. 3.4 Turbulent statistics compared with the experimental result

4. DISPERSION PLUMES FROM A POINT SOURCE IN URBAN-LIKE AREA

4.1 Analysis condition of dispersion plume model

To reveal the complex mechanism of mechanical roughness effect by city, atmospheric stability effect, local thermal effect, we performed plume dispersion analysis by LES using urban canopy model simplified by cubic shaped blocks which have thermal condition on the wall surfaces (Fig. 4.1). Table 4.1 shows thermal condition of all cases. The solar radiation heating of the wall surface at daytime is assumed as case3, the radiative cooling of the roof surface at the winter night is assumed as case4. Computational domain is x: $7.5\delta_0$, y: $5\delta_0$, z: $7.5\delta_0$, boundary conditions are similar to Driver region 2. Setting of point source on diffusion material is also shown in Fig. 4.1. Inflow boundary condition in Driver region 3 used the temperature and velocity of inflow turbulence which was produced in Driver region 2, including the thermal stratification effect.

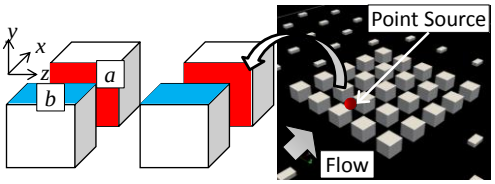

building coverage :25%
number of blocks :25
height :$0.2\delta_0$=40m
shape :cube

Fig. 4.1 Condition of urban canopy model

Table 4.1 Analysis condition of each case

	stability $g\beta(\theta_\infty - \theta_s)$	surface temperature θ_s	dair temperature θ_∞	wall temperature
case1	0	0	0	adiabatic
case2	110.5	0	1	adiabatic
case3	110.5	0	1	upwind(a): 1 downwind: 0
case4	110.5	0	1	roof surface(b):-1

4.2 General results of plume dispersion model

Fig. 4.2 shows the averaged concentration field, Fig. 4.3 shows the averaged temperature field, Fig. 4.4 shows the averaged velocity vector inside the canyon on each case, Fig. 4.5 shows the averaged temperature field of case2 and case4. Firstly we discuss about case1 and case2 which have different stratification effect. Diffusion width of concentration is reduced by stable stratification effect and, high concentration area extends to downstream. This means the stratification effect which is produced in previous section also appears in the diffusion characteristics. The temperature field in case2, low-temperature region near ground surface expands in a wider region because of decreased wind velocity inside the canyon by the stratification effect.

In case2 and case3, there is not large difference. However, diffusion height in the vertical direction is reduced in case3. This means the reduction of vortex strength since the buoyancy effect caused by heated wall inhibits the upward flow.

In case4, there is a large difference with the other cases. The high concentration area near the ground by stratification effect move upward in Fig. 4.2. Downward flow dominates in the canyon shown in Fig. 4.3. Then, cold air at roof surface is advected downward, the canyon inside become also cold. This kind of phenomenon is already shown as observation by Moriwaki et al. [(9)]. However, in this study, cold air advection flows strongly crash at downstream wall, descends toward the inside canyon. Therefore, it seems essentially different from the gravitational depression mechanism oresented by Moriwaki's. The 3°C of temperature on this study is realistic compared with Moriwaki's observation. Therefore, this phenomenon is regarded real.

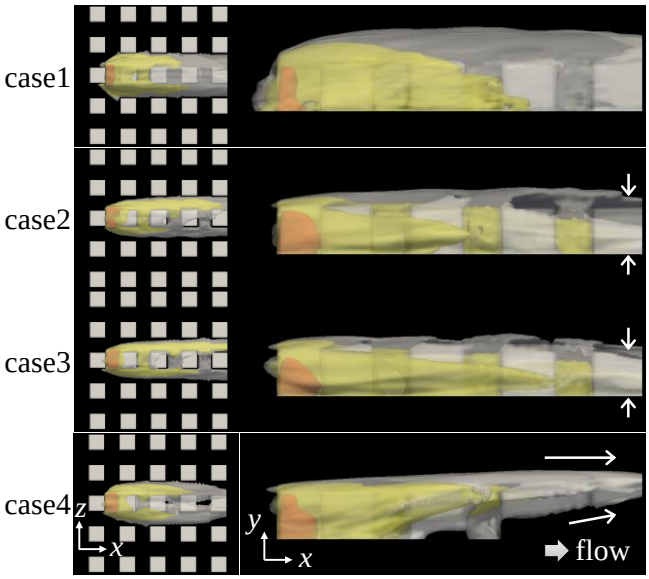

Fig. 4.2 Average of concentration field (red: 0.01, yellow; 0.001, white; 0.0005)

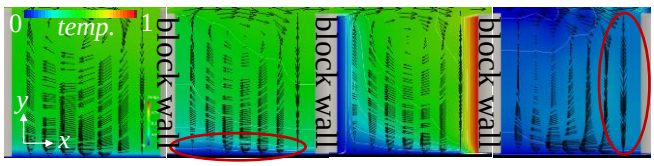

Fig. 4.3 Average of temperature inside the canyon

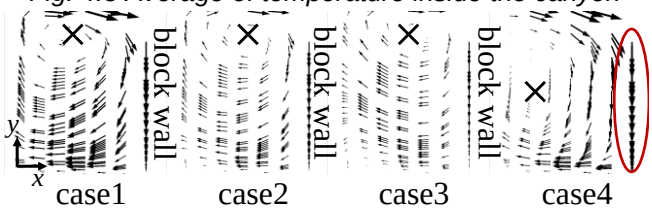

Fig. 4.4 Average of velocity vector inside the canyon (×; vortex core)

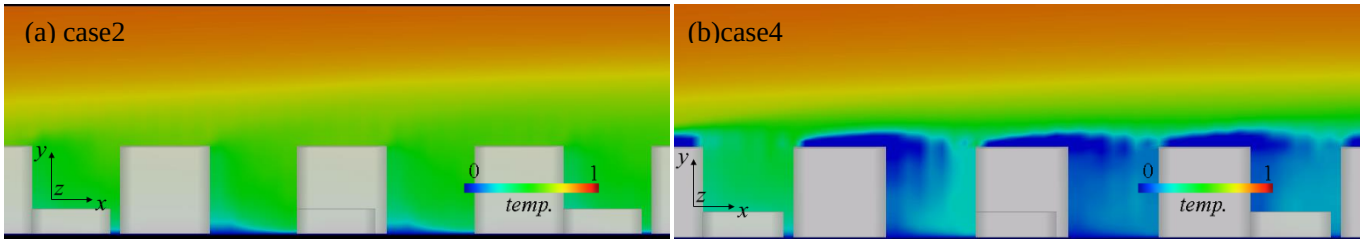

Fig. 4.5 Average temperature field of case2, case4

4.3 Validation of plume dispersion model

Fig. 4.6 shows the comparison of turbulent statistics inside the canopy with the wind tunnel experiment by Uehara et al.[10]. Considering the geometric configuration of their experimental model is similar to this study. These characteristics are reproduced qualitatively by the numerical simulation at neutral condition. In case2, fluctuation amount is decreasing within and without canopy because of thermal stratification effect. There are no differences between case2 and case3, but in case4, fluctuation strength is greatly reduced. This means decrease of Reynolds stress directly affects the large-scale turbulence structure in upper canopy area.

4.4 Vortex structure and transport structure of the diffusion plume

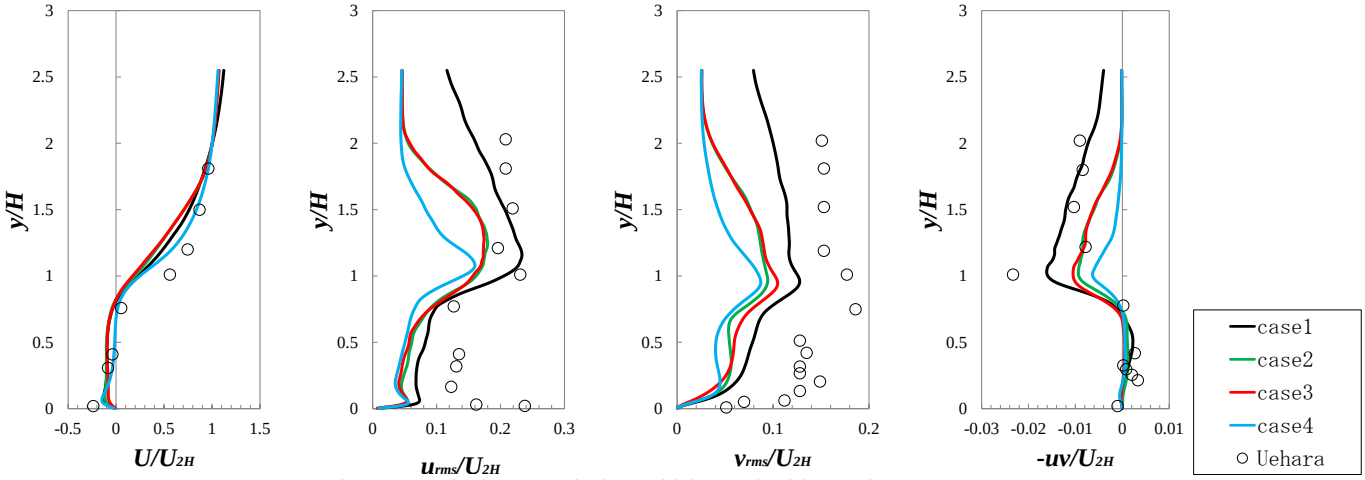

Fig. 4.6 turbulent statistics within and without the canopy area

Fig 4.7 shows vortex structure using Q value (Q=1000) obtained based on mean velocity, where red and blue colors, respectively, mean positive and negative vertical or horizontal vortices. Two types of three-dimensional vortices, i.e., cavity vortex and separation vortex are universally distributed because of uniformly-arranged canyon shape. Most of previous studies focus on the two-dimensional structures, but there are three-dimensional rolled structures in reality.

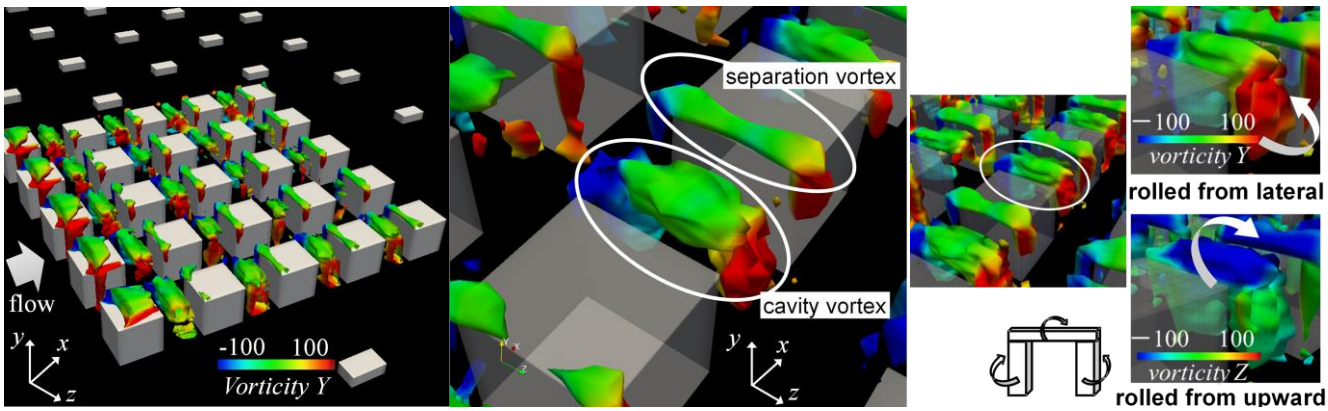

Fig 4.7 Vortex structure using Q value of mean velocity (Q=1000)

In order to consider the relation between roll-shaped cavity vortex and diffusion plume, time series of instantaneous concentration (behind the third rows from the front, center, near the ground, y/δ =0.01) and three-dimensional cavity vortex structure is shown in Fig 4.8. The red circles are sharp peak of high concentration and the red arrows are three dimensional passing structures of diffusion plume. When the large amount of the diffusion material created by inflow turbulence is passing through a canyon side, diffusion plume is brought into the canyon inside because of cavity structure. All of those instantaneous concentration peaks and rolled structure into the interior canyon are temporal coincidence; it can be said that the cavity vortex structure causes the high concentration of diffusion plume.

Time-series of instantaneous concentration of each case is also shown in Fig. 4.8. All of the high concentration peaks are temporally coincidence with the cavity vortex rolled structure also in those cases. However, case2 and case3 include the thermal stratifications and hence the peak concentrations are not as sharp as case1. These differences mean retention time of concentration on each case; it is longer in thermal stratification cases than neutral condition. This implies that the fluid movement towards the canyon is inhibited by stratification effect.

In case4, fluid movement is activated and wave profile is similar to case1, because of low temperature on the canyon inside cases advection of cold air.

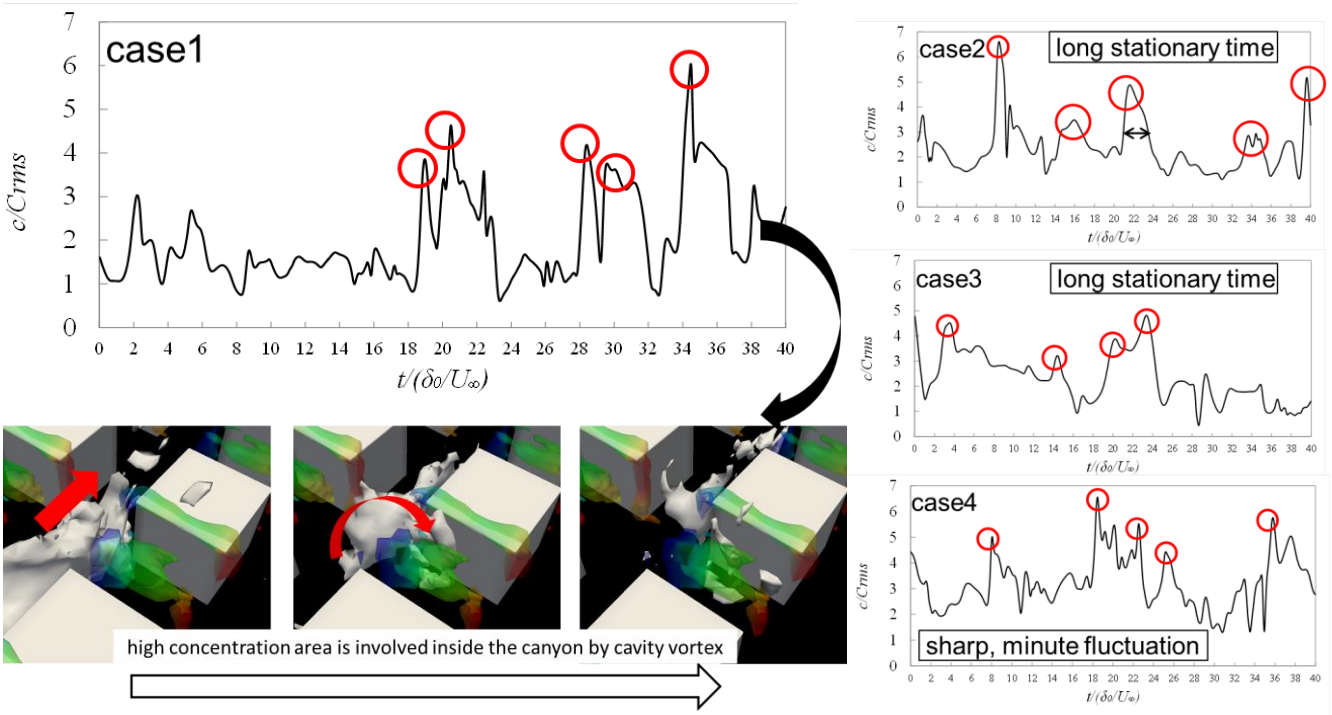

Fig 4.8 Instantaneous concentration and three-dimensional cavity vortex

5 CONCLUSION

1. We validate the adequacy of inflow turbulence including the thermal stratification effect generated in this study, based on the comparison with Ohya's experimental results.
2. It is important to consider the roughness effect near the ground for heat and momentum transportation under the stable condition.
3. Comparing the thermal stability conditions with local thermal effect, we found that the large impact on the behavior of mean concentration by the local thermal effect on building walls.
4. From the flow visualization, three-dimensional cavity vortex structures universally exist inside the canyon, and these rolled structures contribute to the high concentration peaks inside the canyon.

References

(1) Michioka T., Takimoto H., Sato A., 2014; Large-Eddy Simulation of Pollutant Removal from a Three-Dimensional Street Canyon, *Boundary-Layer Meteorology*. **150**, 259–275.
(2) Xian-Xiang Li, Rex E. Britter, Leslie K. Norford, Tieh-Yong Koh, Dara Entekhabi, (2012); Flow and Pollutant Transport in Urban Street Canyons of Different Aspect Ratios with Ground Heating : Large-Eddy Simulation, *Boundary-Layer Meteorology*, **142**, 289–304.
(3) Nozawa K., Tamura T.,2008; Large Eddy Simulation of a Turbulent Boundary Layer Flow over Urban-Like Roughness, *IUTAM Bookseries,* **4**, 285–290.
(4) Lund, T.S., Wu, X., and Squires, K.D., 1998; Generation of turbulent inflow data for spatially-developing boundary layer simulations, *J. Comput. Phys.*, **140**, 233–258.
(5) Goldstein, D., Handler, R., and Sirovich, L.,1993; Modeling a no-slip flow boundary with an external force field, *J. Comput. Phys.*, **105**, 354–366.
(6) Schultz M.P. and Flack K.A., 2007; The rough-wall turbulent boundary layer from the hydraulically smooth to the fully rough regime, *J.Fluid Mech*., **580**, 381–405
(7) Architectural Institute of Japan, 2004; Load Recommendation for Building Design, Japanese.
(8) Ohya, Y. et al., 1997; Turbulence structure in a stratified boundary layer under stable conditions, *Boundary-Layer Meteorology*. **83**, 139–161.
(9) Kanda M., Moriwaki R., Kasamatsu F., 2006; Spatial variability of turbulent fluxes and temperature profile in an urban roughness layer, *Boundary-Layer Meteorology*, **121**, 339–350.
(10) Uehara, K., Murakami, S., Oikawa, S., Wakamatsu, S., 2000; Wind tunnel experiments on how thermal stratification affects flow in and above urban street canyons, *Atmos. Environ.*, **34**, 1553–1562.